Hindawi Publishing Corporation
Journal of Nanomaterials
Volume 2015, Article ID 492657, 7 pages
http://dx.doi.org/10.1155/2015/492657

Research Article

Fabrication and Characterization of CNT-Based Smart Tips for Synchrotron Assisted STM

Hui Yan,[1,2] Marvin Cummings,[3] Fernando Camino,[4] Weihe Xu,[1] Ming Lu,[4] Xiao Tong,[4] Nozomi Shirato,[3] Daniel Rosenmann,[3] Volker Rose,[3] and Evgeny Nazaretski[1]

[1]*Brookhaven National Laboratory, 2 Center Street, Upton, NY 11973, USA*
[2]*University of Louisiana at Lafayette, Lafayette, LA 70504, USA*
[3]*Argonne National Laboratory, 9700 S. Cass Avenue, Argonne, IL 60439, USA*
[4]*Center for Functional Nanomaterials, Brookhaven National Laboratory, 2 Center Street, Upton, NY 11973, USA*

Correspondence should be addressed to Hui Yan; huiyan@louisiana.edu and Evgeny Nazaretski; enazaretski@bnl.gov

Received 29 May 2015; Accepted 5 August 2015

Academic Editor: Ya Yang

Determination of chemical composition along with imaging at the atomic level provides critical information towards fundamental understanding of the surface of materials and, hence, yields the capability to design new materials by tailoring their ultimate functionalities. Synchrotron X-ray assisted scanning tunneling microscopy (SX-STM) is a promising new technique to achieve real space chemically specific atomic mapping. Chemical sensitivity of SX-STM relies on excitation of core electrons by incident X-rays when their energy is tuned to an absorption edge of a particular element. However, along with core-level electrons, photoelectrons are also excited, which yield additional current and interfere with the tunneling current. To reduce the background photoelectron current and to improve ultimate resolution of SX-STM, we have developed and fabricated multiwalled carbon nanotubes (MWCNT) based "smart tips" using plasma enhanced chemical vapor deposition and focused ion beam milling. The newly developed CNT-based smart tips, characterized step by step by scanning electron microscopy (SEM) during the fabrication process, demonstrate good performance and provide opportunity for realizing atomic chemical mapping.

1. Introduction

Precise determination of atomic structure and chemical composition of complex materials, especially at interfaces, allows engineering and developing of material systems with specific physical properties and functionalities. Scanning tunneling microscopy (STM) is a standard tool to atomically resolve surface topography and perform spectroscopic measurements on various conductive materials systems [1, 2]. The limitation of conventional STM pertains to the fact that it probes electrons in the valence or conduction bands only but does not provide any chemical information of a surface. The concept of combining STM technique with chemical sensitivity has been proposed and culminated in the development of a synchrotron X-ray assisted STM (SX-STM) [3–5]. Chemical sensitivity of SX-STM relies on excitation of core electrons by incident X-rays when their energy is tuned to an absorption edge of a particular element on the surface. However, along with core-level electrons, photoelectrons including primary and secondary Auger electrons and secondary photoelectrons from the sample surface are also excited and collected by a tip. Moreover, STM tip itself is also exposed to X-rays since typically the size of a tip apex is much smaller than the spot size of an incident X-ray beam, that is, submicrometer compared to micrometer. The STM tip cannot distinguish between different electronic contributions but collects current originating from both tunneling itself and current stimulated by photoemission. Photoemission processes interfere with quantum tunneling and introduce the background onset, making detection of chemically specific tunneling difficult. One of the routes to reduce photoelectron current is to minimize surface area of STM tip that is capable of detecting photoelectrons, that is, to fabricate a "smart tip." A smart tip refers to a tip that

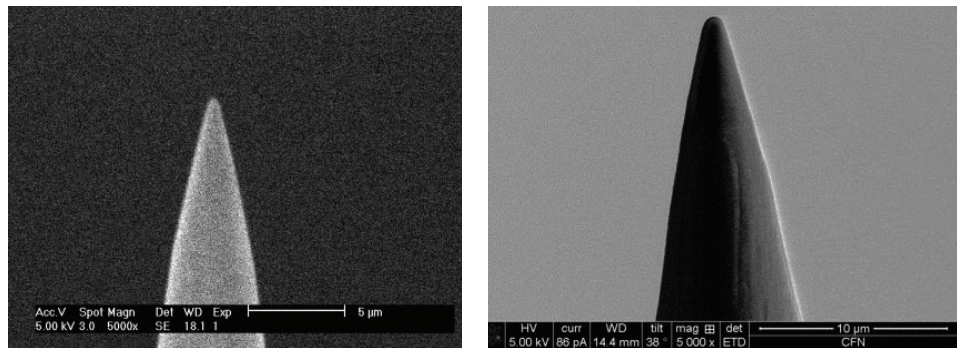

(a) (b)

Figure 1: Scanning electron micrograph (SEM) images of an electrochemically etched $Pt_{90}Ir_{10}$ tip before (a) and after (b) being coated with 230 nm SiO_2 by PECVD.

is entirely coated by insulating film except for a tip apex. The insulating film helps to minimize the background signals introduced by photoejected electrons collected through the sidewalls of a tip. Glass coated tungsten (W) and silica (SiO_2) coated W tips have been fabricated [6, 7] and 10 nm spatial resolution has been achieved; however, W oxidizes rapidly during the fabrication process. Other developments of smart tips focused on fabrication of PtIr tips due to the chemical inertness of PtIr. To form an insulating layer, PtIr tips have been coated with boron nitride (BN) by dipping in BN solution or coated with SiO_2 by e-beam deposition [5, 8, 9]. Most recently, more sophisticated coaxial metal-insulator-metal smart tips have been utilized and exhibited enhanced chemically specific spatial resolution of 2 nm [10].

Complimentary to recent achievements in tip fabrication techniques, we propose an alternative approach to fabricate smart tips based on carbon nanotube (CNT). The potential advantage of CNT-based smart tips is a better knowledge of the tip p orbitals contributing to the tunneling process, as compared to sometimes undefined orbitals in metallic tips. In addition, CNTs are chemically inert to oxygen and water, while having interesting physical properties (stiff, superior elastic properties, with maximum Young's module of ~1 TPa and tensile strength of 63 GPa [11]). They are suitable for fabrication and STM imaging. Furthermore, CNTs can be chemically functionalized at their ends with various functionalities, allowing chemically selective STM image based on charge-transfer interaction [12]. CNTs attached to or grown on tungsten tips have been successfully used for STM applications and demonstrated subnanometer resolution of topographic features [13–15]. The large aspect ratio of CNT is potentially also beneficial for SX-STM studies, resulting from small area being exposed to X-rays. In present work, we report details of the fabrication and characterization followed by performance evaluation of CNT-based smart tips, for the first time. This work is a significant step toward successful application of CNT-based "smart tips" for SX-STM experiments.

2. Experiment

Multiwalled CNT (MWCNT, the ones used in this work and spelled out as "CNTs" for abbreviation) attached to SiO_2 coated $Pt_{90}Ir_{10}$ tip with submicron conducting apex were prepared by means of plasma enhanced chemical vapor deposition (PECVD), focused ion beam milling (FIB), and subsequent electron beam stimulated oxide growth. A step by step characterization of smart tips was performed using SEM (Helios dual beam SEM-FIB) during and after the tip fabrication process.

2.1. SiO_2 Coating. Tips were electrochemically etched from a clean $Pt_{90}Ir_{10}$ wire with a diameter of 0.250 mm (99.999%, Alfa Aesar) using 1.5 M $CaCl_2$ (≥96%, Fisher Scientific) solutions, to form a sharp and symmetric apex (Figure 1(a)). The electrochemically etched $Pt_{90}Ir_{10}$ wire has a radius of curvature smaller than 200 nm, typically, 100 nm. After cleaning with hot deionized water and methanol, SiO_2 films with various thickness, 100 nm–3 μm, were deposited on the wires by PECVD (Trion Orion III), through a recipe with the flow ratio of $SiH_4 : N_2 : N_2O = 86 : 100 : 100$, at 980 Torr, 400°C, and 60 W RF power. The thickness of SiO_2 was controlled by the process time. In order to assure uniform coating, the tips were flipped every 50 nm deposition at a deposition rate of 2 nm/s. Figure 1 shows scanning electron micrograph (SEM) images of $Pt_{90}Ir_{10}$ before and after the deposition of the oxide film. After deposition, the entire tip was coated with a 230 nm SiO_2 insulating film, which extends to the area above the tip.

2.2. Exposure of the Conductive $Pt_{90}Ir_{10}$ Pillar. In order to remove oxide at the tip apex and to expose the conductive part for CNT attachment, a two-step FIB (Helios dual beam SEM-FIB, FEI Company) process was applied to fabricate the tips. First, Ga^+ ions from FIB (30 keV, 90 pA) were impinged normal to the tip axis, to expose the radial cross section of the tip apex. A SEM image of a top view of the radial cross section for a 570 nm SiO_2-$Pt_{90}Ir_{10}$ tip is shown in Figure 2(a). Second, Ga^+ ions (30 keV, 9–90 pA) were impinged at normal incidence to the radial cross section, and then a series of donut-shape writing patterns, with decreasing diameter and ion beam current, from FIB were used to fabricate a $Pt_{90}Ir_{10}$ pillar, as shown in Figures 2(b)–2(e). Typically, a $Pt_{90}Ir_{10}$ pillar with 1 μm in length and 200 nm in average diameter can be fabricated. For example, for a 570 nm SiO_2 coated $Pt_{90}Ir_{10}$

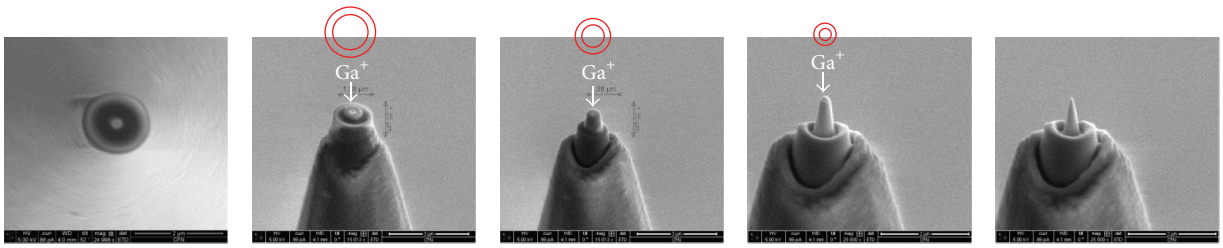

FIGURE 2: SEM images of the radial cross section (top view) of a 570 nm SiO_2-$Pt_{90}Ir_{10}$ tip (a); during focused ion beam (FIB) fabrication using circular/donut-shape pattern (b–e), tip was placed parallel to ion beam and 52° from electron beam. About 1 μm long $Pt_{90}Ir_{10}$ pillar with a radius of curvature less than 100 nm was exposed after fabrication.

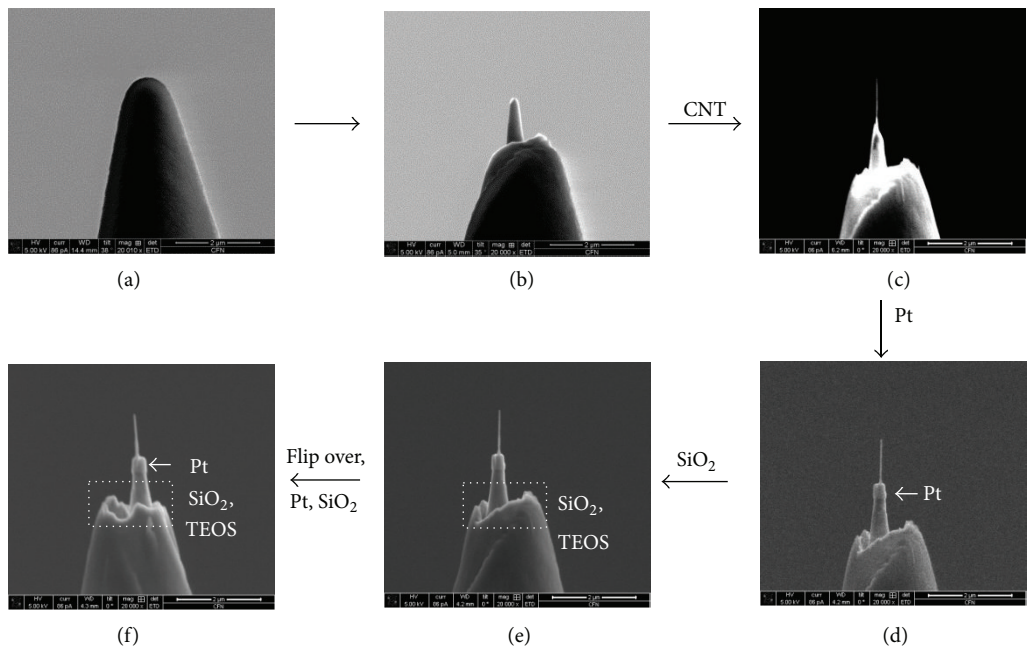

FIGURE 3: SEM images of a CNT-based smart tip during the fabrication process: (a) $Pt_{90}Ir_{10}$ with 230 nm thick SiO_2 film formed from PECVD; (b) fabricated to expose a 1.2 μm long $Pt_{90}Ir_{10}$ pillar; (c) attached with a CNT (580 nm in length and 20 nm in diameter); (d) deposited with 70 nm thick Pt on the contact of CNT with $Pt_{90}Ir_{10}$ pillar; (e) recovered with 50 nm thick SiO_2 by localized electron beam assisted CVD of TEOS on the area shown in dashed rectangle; and (f) flipped over and deposited with Pt and recovered with SiO_2.

tip in Figure 2, ion milling results in a 1 μm long $Pt_{90}Ir_{10}$ pillar with a radius of curvature less than 100 nm. Another example is shown in Figures 3(a) and 3(b).

2.3. CNT Attachment and SiO_2 Film Recovery. Due to inertness of $Pt_{90}Ir_{10}$ wire, pillar preserved its shape and properties prior to CNT attachment. The fabricated $Pt_{90}Ir_{10}$ tip was then mounted on a micromanipulator as part of a conductive circuit inside a dedicated SEM. By applying a small DC voltage to both CNT and pillar and due to electrostatic force, a CNT of interest was brought to the $Pt_{90}Ir_{10}$ tip and then aligned normally to the tip apex, as straight as possible. Subsequently, higher power was applied to ensure welding of CNT to the tip. A fabricated $Pt_{90}Ir_{10}$ tip with 230 nm SiO_2 (shown in Figures 1(b) and 3(a)) and 1.2 μm $Pt_{90}Ir_{10}$ pillar (Figure 3(b)) is used to illustrate the attachment of CNT (Figure 3(c)) and the repair of SiO_2 film (Figures 3(e)-3(f)) in Figure 3. Figure 3(c) shows the successful attachment of a CNT, 580 nm in length and 20 nm in diameter, to the fabricated pillar. The contact of CNT with $Pt_{90}Ir_{10}$ pillar was further strengthened by localized Pt deposition from ion beam assisted CVD (FIB), as shown in Figures 3(c) and 3(f). Only CNT is expected to be exposed to X-ray illumination and the exposed area of $Pt_{90}Ir_{10}$ pillar to the X-ray must be limited. This was accomplished by localized growth of an insulating film through electron beam assisted chemical vapor deposition, using tetraethyl orthosilicate ($Si(OC_2H_5)_4$, TEOS), a precursor molecule for SiO_2. TEOS was applied in situ through a nozzle in close proximity to the tip, along with H_2O. The interactions of the precursor molecules with high energy electrons caused the deposition of an insulating film in areas where the electrons were hitting the tip. After multiple

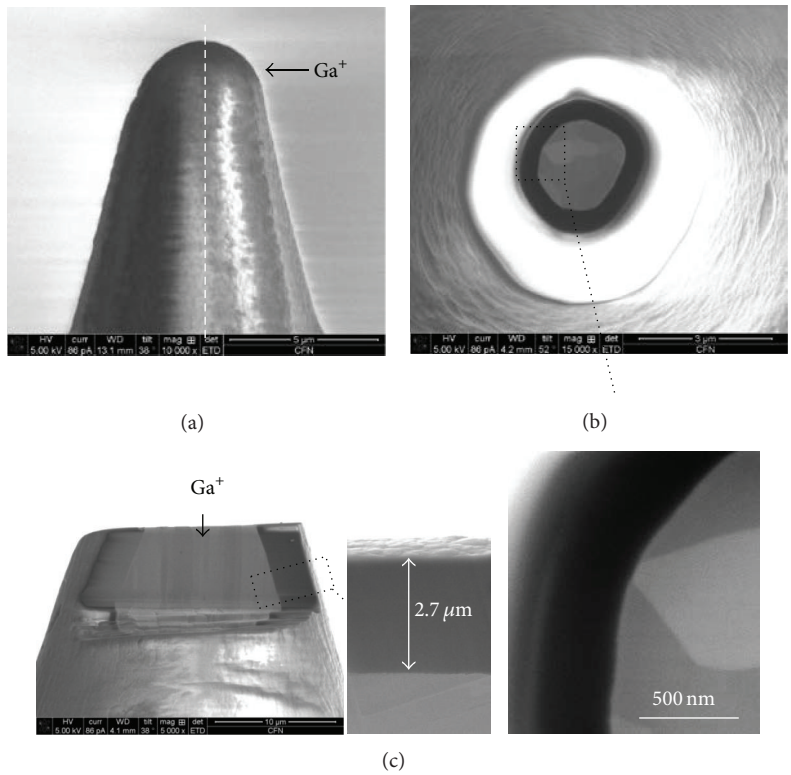

Figure 4: (a) Scanning electron micrographs (SEM) of a $Pt_{90}Ir_{10}$ tip coated with 2.7 μm SiO_2 by PECVD; (b) the radial cross section of the tip apex and zoom-in image of the area in dashed square; and (c) the sidewall cross section along the tip axis and its zoom-in image in dashed rectangle.

iterations, including rotation/flipping of the tip along the tip axis, a CNT attached to a submicron exposed apex of a SiO_2 coated tip was obtained. A recovered 50 nm SiO_2 layer is shown in Figures 3(e)-3(f). Lower part of CNT was also coated with 5–10 nm thick silica due to the deposition from residue TEOS in the chamber.

3. Results and Discussion

3.1. Quality of SiO_2 Film. In order to investigate SiO_2 film quality, a thick 2.7 μm SiO_2 film is deposited to a $Pt_{90}Ir_{10}$ wire (Figure 4(a)) and then focused ion beam (FIB) is applied to the tip with Ga^+ ions impinging at normal incidence to the tip axis (white dash line in Figure 4(a)) to obtain the radial cross section of the tip. A closed SiO_2 film with a thickness of 2.7 μm is observed in Figure 4(b). The film replicates shape of the electrochemically etched $Pt_{90}Ir_{10}$ wire very well. Despite changing contrast from charging due to the thick insulating layer, the film looks even and rigid, which is confirmed by an image of the enlarged area. The zoom-in image also displays the interface between SiO_2 and $Pt_{90}Ir_{10}$, where no void or gaps are observed and the SiO_2 film sticks to $Pt_{90}Ir_{10}$ wire seamlessly. To evaluate the quality of the film along the sidewall, Ga^+ ions are impinged parallel to the tip axis. Figure 4(c) shows that the cross section has distinct contrast between SiO_2 and $Pt_{90}Ir_{10}$ signals, suggesting clear boundary between SiO_2 and $Pt_{90}Ir_{10}$. The film growth is very uniform along the sidewalls of the tip. No void is observed in the oxide part of the tip and interface between SiO_2 and $Pt_{90}Ir_{10}$ is seamless; therefore, it is legitimate to conclude that quality of SiO_2 formed by PECVD is high. Furthermore, chemical compositions of the SiO_2 layer formed by PECVD and the recovered layer by TEOS are determined to be $SiO_{2.37}$ and $SiO_{2.66}$, respectively, by energy dispersive spectroscopy, suggesting the films formed by two methods are comparable in chemical compositions.

3.2. Performance. In order to evaluate performance of developed smart tips, we used a CNT-based tip for scanning on a freshly cleaved highly oriented pyrolytic graphite (HOPG) surface in air. HOPG was chosen for the ease of handling as a model surface. The smart tip was used as prepared without further conditioning. STM scan was carried out at +200 mV sample bias with the tunneling current of 0.5 nA in a constant current mode; we used Veeco Multimode V SPM system for characterization measurements. As shown in Figure 5, STM image of HOPG taken in air (Figure 5(a)) with corresponding line profiles extracted from the image (Figure 5(b)) exhibits resolution of single atomic layer, with the step height of 3.4 ± 1.8 Å [16], double layer (6.7 Å), and 4-layer (13.4 Å) steps on HOPG.

To further evaluate performance of CNT-based tips and understand their response to the incident X-ray beam, smart tip has been installed in the SX-STM-V2 system [17] at

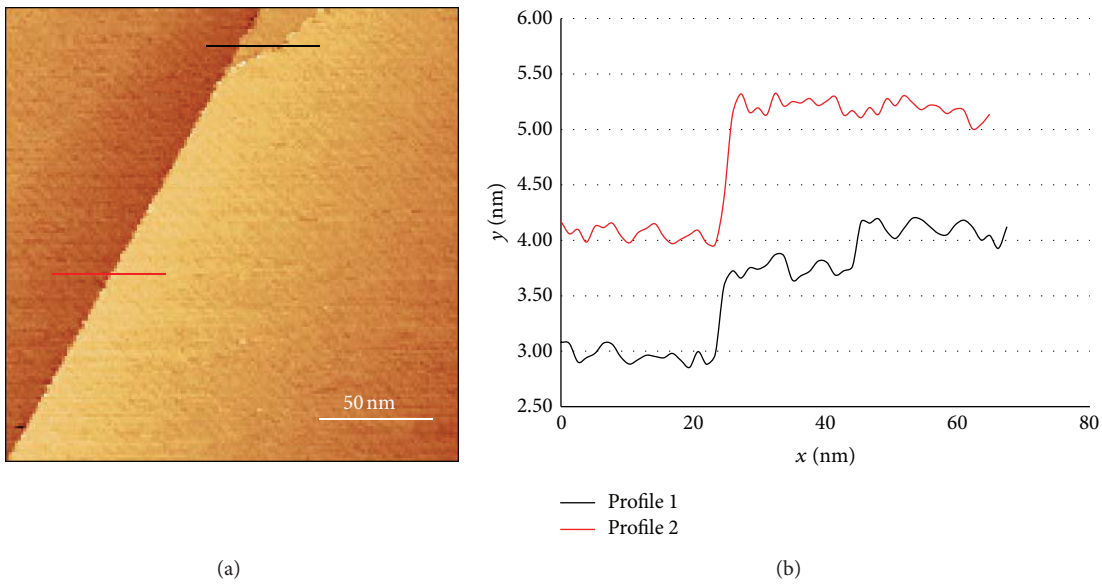

FIGURE 5: (a) STM image on HOPG (200 nm × 200 nm) in air, scanning parameters $I_{tunneling}$ = 0.5 nA, U_{bias} = +200 mV; (b) line profiles of the image, single and double atomic layers in black and 4 atomic layers in red.

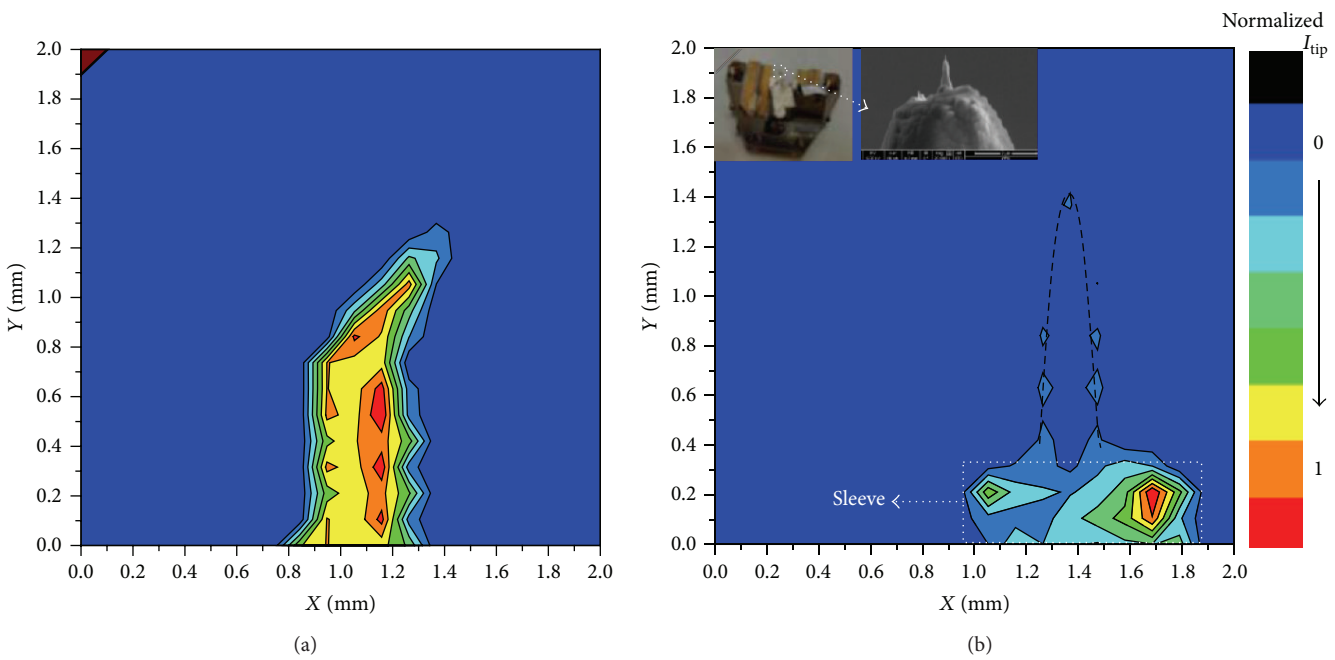

FIGURE 6: (a) Normalized photocurrent map of the bare $Pt_{90}Ir_{10}$ tip (0.5 mm in diameter). The photocurrent is normalized with respect to the maximum current detected in the same plot; (b) normalized photocurrent map of a CNT-based smart tip (0.25 mm $Pt_{90}Ir_{10}$ wire coated with 350 nm SiO_2, attached to a CNT, as shown in the insert). A thick boron nitrite film is applied to the tip holder to additionally reduce the photocurrent. The black dash line is used as a guide to show where the tip apex is. The result shows that photocurrent is generated by the whole bare tip apex while the photocurrent of the smart tip is drastically reduced after coating the tip with SiO_2.

beamline 26-ID of the Advanced Photon Source [18]. The efficiency of coatings has been evaluated and compared with a bare $Pt_{90}Ir_{10}$ reference tip. Tips were mounted on a titanium tip holder with a 1.0 mm sleeve (insert of Figure 6(b)) and then exposed to X-rays at photon energy of 9000 eV, slightly over Cu K absorption edge. When X-rays hit the tip, absorption leads to ejection of photoelectrons. The charge flow that is needed to keep the grounded tip neutral is recorded as photocurrent. A photocurrent map is derived from scanning the tip holder through the stationary X-ray beam of approximately 100 × 100 μm^2. The photocurrent detected by the tip, I_{tip}, is collected and then normalized to the maximum value in that same scan. Figure 6 depicts the contour maps of the normalized tip current for a bare

reference tip and a CNT-based smart tip, respectively. For the bare $Pt_{90}Ir_{10}$ tip, photocurrent is generated by almost every part of the tip, as shown in Figure 6(a). A photograph and an SEM image of a fabricated smart tip, coated with 350 nm SiO_2 from PECVD and equipped with a CNT of 230 nm in length and 20 nm in diameter, are shown in Figure 6(b). The titanium tip holder in Figure 6(b) is coated with a thick insulating boron nitride film, which further reduces the background photocurrent originating from the tip holder itself. As shown in Figure 6(b), the current generated by the tip apex part is significantly lower than signals recorded by the less uniform BN coated tip holder (the sleeve, white dashed box in Figure 6(b)). This suggests that SiO_2 layer, deposited on metal tips, suppresses the background photoelectron current and enables chemically specific STM measurement.

4. Conclusions

In conclusion, we have applied a combination of PECVD and FIB to fabricate CNT-based smart tips, which are core components of synchrotron assisted STM. The SiO_2 coating formed from PECVD and repaired by TEOS is rigid and uniform and strongly reduces the number of photoejected electrons. Results of our work indicate that the development of nanoscale diameter CNT attached to insulator-coated metal tips is a promising venue for applications in synchrotron-based scanning probe microscopy. When used in conjunction with a topographic filter [19], developed tips can be potentially applied for atomic imaging and spectroscopy with chemical, electronic, and magnetic contrast.

Conflict of Interests

The authors declare that there is no conflict of interests regarding the publication of this paper.

Acknowledgments

This research used resources of the Center for Functional Nanomaterials, which is U. S. DOE Office of Science User Facility, at Brookhaven National Laboratory under Contract no. DE-SC0012704. Work at the Advanced Photon Source and the Center for Nanoscale Materials was supported by the U. S. Department of Energy, Office of Science, Office of Basic Energy Sciences, under Contract no. DE-AC02-06CH11357, and the Office of Science Early Career Research Program through the Division of Scientific User Facilities, Office of Basic Energy Sciences, U. S. Department of Energy, through Grant SC70705. The authors would like to thank Carbon Design Innovations, Inc. for CNT attachment.

References

[1] G. Binnig, H. Rohrer, C. Gerber, and E. Weibel, "Tunneling through a controllable vacuum gap," *Applied Physics Letters*, vol. 40, no. 2, pp. 178–180, 1982.

[2] G. Binnig and H. Rohrer, "Scanning tunneling microscopy," *IBM Journal of Research and Development*, vol. 30, no. 4, pp. 355–369, 1986.

[3] T. Matsushima, T. Okuda, T. Eguchi et al., "Development and trial measurement of synchrotron-radiation-light-illuminated scanning tunneling microscope," *Review of Scientific Instruments*, vol. 75, no. 6, pp. 2149–2153, 2004.

[4] A. Saito, J. Maruyama, K. Manabe et al., "Development of a scanning tunneling microscope for in situ experiments with a synchrotron radiation hard-X-ray microbeam," *Journal of Synchrotron Radiation*, vol. 13, no. 2, pp. 216–220, 2006.

[5] V. Rose, J. W. Freeland, K. E. Gray, and S. K. Streiffer, "X-ray-excited photoelectron detection using a scanning tunneling microscope," *Applied Physics Letters*, vol. 92, no. 19, Article ID 193510, 4 pages, 2008.

[6] K. Akiyama, T. Eguchi, T. An et al., "Fabrication of a glass-coated metal tip for synchrotron-radiation-light- irradiated scanning tunneling microscopy," *Review of Scientific Instruments*, vol. 76, no. 8, Article ID 083711, 2005.

[7] A. Saito, K. Takahashi, Y. Takagi et al., "Study for noise reduction in synchrotron radiation based scanning tunneling microscopy by developing insulator-coat tip," *Surface Science*, vol. 601, no. 22, pp. 5294–5299, 2007.

[8] V. Rose, K. Wang, T. Chien et al., "Synchrotron X-ray scanning tunneling microscopy: fingerprinting near to far field transitions on Cu(111) induced by synchrotron radiation," *Advanced Functional Materials*, vol. 23, no. 20, pp. 2646–2652, 2013.

[9] V. Rose, T. Y. Chien, J. Hiller, D. Rosenmann, and R. P. Winarski, "X-ray nanotomography of SiO_2-coated $Pt_{90}Ir_{10}$ tips with sub-micron conducting apex," *Applied Physics Letters*, vol. 99, no. 17, Article ID 173102, 3 pages, 2011.

[10] N. Shirato, M. Cummings, H. Kersell et al., "Elemental fingerprinting of materials with sensitivity at the atomic limit," *Nano Letters*, vol. 14, no. 11, pp. 6499–6504, 2014.

[11] M.-F. Yu, O. Lourie, M. J. Dyer, K. Moloni, T. F. Kelly, and R. S. Ruoff, "Strength and breaking mechanism of multiwalled carbon nanotubes under tensile load," *Science*, vol. 287, no. 5453, pp. 637–640, 2000.

[12] T. Nishino, T. Ito, and Y. Umezawa, "Carbon nanotube scanning tunneling microscopy tips for chemically selective imaging," *Analytical Chemistry*, vol. 74, no. 16, pp. 4275–4278, 2002.

[13] T. Shimizu, H. Tokumoto, S. Akita, and Y. Nakayama, "Stable atomic imaging of Si(1 1 1)-7 × 7 surface by scanning tunneling microscope with carbon nanotube tip," *Surface Science*, vol. 486, no. 3, pp. L455–L460, 2001.

[14] S. Kim, J. Kim, M. Berg, and A. de Lozanne, "Robust Ohmic contact junctions between metallic tips and multiwalled carbon nanotubes for scanned probe microscopy," *Review of Scientific Instruments*, vol. 79, Article ID 103702, 5 pages, 2008.

[15] F.-K. Tung, M. Yoshimura, and K. Ueda, "Direct fabrication of carbon nanotubes STM tips by liquid catalyst-assisted microwave plasma-enhanced chemical vapor deposition," *Journal of Nanomaterials*, vol. 2009, Article ID 612549, 6 pages, 2009.

[16] H. Chang and A. J. Bard, "Observation and characterization by scanning tunneling microscopy of structures generated by cleaving highly oriented pyrolytic graphite," *Langmuir*, vol. 7, no. 6, pp. 1143–1153, 1991.

[17] M. L. Cummings, T. Y. Chien, C. Preissner et al., "Combining scanning tunneling microscopy and synchrotron radiation for high-resolution imaging and spectroscopy with chemical, electronic, and magnetic contrast," *Ultramicroscopy*, vol. 112, pp. 22–31, 2012.

[18] R. P. Winarski, M. V. Holt, V. Rose et al., "A hard X-ray nanoprobe beamline for nanoscale microscopy," *Journal of Synchrotron Radiation*, vol. 19, no. 6, pp. 1056–1060, 2012.

[19] K. Wang, D. Rosenmann, M. Holt, R. Winarski, S.-W. Hla, and V. Rose, "An easy-to-implement filter for separating photo-excited signals from topography in scanning tunneling microscopy," *Review of Scientific Instruments*, vol. 84, no. 6, Article ID 063704, 4 pages, 2013.